International Journal of Minerals, Metallurgy and Materials
Volume 22, Number 4, April 2015, Page 389
DOI: 10.1007/s12613-015-1084-0

Solid fraction evolution characteristics of semi-solid A356 alloy and *in-situ* A356–TiB_2 composites investigated by differential thermal analysis

S. Deepak Kumar[1)], *A. Mandal*[2)], *and M. Chakraborty*[2)]

1) School of Mechanical Sciences, Indian Institute of Technology Bhubaneswar, Bhubaneswar - 751013, Odisha, India

2) School of Minerals, Metallurgical and Materials Engineering, Indian Institute of Technology Bhubaneswar, Bhubaneswar - 751007, Odisha, India

(Received: 22 June 2014; revised: 7 August 2014; accepted: 3 September 2014)

Abstract: The key factor in semi-solid metal processing is the solid fraction at the forming temperature because it affects the microstructure and mechanical properties of the thixoformed components. Though an enormous amount of data exists on the solid fraction–temperature relationship in A356 alloy, information regarding the solid fraction evolution characteristics of A356–TiB_2 composites is scarce. The present article establishes the temperature–solid fraction correlation in A356 alloy and A356–$x$$TiB_2$ (x = 2.5wt% and 5wt%) composites using differential thermal analysis (DTA). The DTA results indicate that the solidification characteristics of the composites exhibited a variation of 2°C and 3°C in liquidus temperatures and a variation of 3°C and 5°C in solidus temperatures with respect to the base alloy. Moreover, the eutectic growth temperature and the solid fraction (f_s) vs. temperature characteristics of the composites were found to be higher than those of the base alloy. The investigation revealed that *in-situ* formed TiB_2 particles in the molten metal introduced more nucleation sites and reduced undercooling.

Keywords: particle reinforced composites; aluminum alloys; titanium boride; casting; solid fraction; differential thermal analysis

1. Introduction

Semi-solid metal processing (SSMP) is an established unique manufacturing process used to form near-net-shape products, particularly for automotive components [1]. Compared to conventional forming processes, SSMP possesses several advantages, such as a higher product quality, lower forming temperature, higher production rate, and significant mechanical properties in the components [2].

The two major routes of SSMP include "rheocasting" and "thixoforming". The production of non-dendritic semi-solid slurry by shearing during solidification and injection of the slurry directly into the die is termed as "rheocasting". Thixoforming, on the other hand, is a two-step process involving the preparation of a feedstock material, and subsequent reheating of the feedstock material to a semi-solid temperature [3]. For both processes, the key parameter is to obtain a feedstock material with nearly spherical primary α-Al particles [4]. The important routes for obtaining non-dendritic feedstock for SSMP [3] include mechanical stirring, magneto-hydrodynamic stirring (MHD), strain induced melt activated (SIMA) process, and the cooling slope (CS) casting process. Amongst these processes, CS casting is a simple rheocasting process to produce non-dendritic feedstock for further processing via the thixoforming route [5–6].

A356 alloy is one of the most widely used alloys for thixoforming because of its excellent casting characteristics, weldability, and corrosion resistance [7–8]. *In-situ* reinforced aluminum based metal matrix composites (AMMCs) have recently emerged as one of the most promising alternatives for eliminating the inherent defects associated with *ex-situ* reinforced AMMCs. Moreover, metal forming in the semi-solid state has gained importance in the manufacturing of AMMCs [9–10]. It has been well reported that AMMCs reinforced with TiB_2 particles show significant improvement in mechanical properties in comparison to the base alloy [11–12].

The performance of AMMCs depends very much on the

Corresponding author: A. Mandal E-mail: animesh@iitbbs.ac.in

solidification behavior, which is dictated by the thermo-physical properties of reinforcement and matrix materials [13]. It was reported by Jeng and Chen [14] that the solidification curve is one of the most important characteristics in solidification processing. Birol [15] subsequently conducted experiments on a semi-solid aluminum alloy, and reported that the solid fraction characteristics at the forming temperature, which play a key role in SSMP, affect the final microstructure and thereby the mechanical properties of the thixoformed components.

Differential thermal analysis (DTA) is one of the thermal analysis techniques used to establish the thermodynamic properties essential in determining the solidification curves of various materials under different heating and cooling rates [16]. Jeng and Chen [14] determined the solidification curves of 6061 and A356 aluminum alloys and their composites reinforced with ceramic particles by employing DTA. They revealed that the principal characteristics of the solidification curves of the composites and their matrix alloy were identical. However, Gowri and Samuel [17] observed that the eutectic growth temperature of composites were higher than that of the base alloy at all cooling rates. Further, the liquidus temperature of the composite melt was lowered by the addition of silicon carbide particles (SiC_p).

Kaufmann *et al.* [18] reported the cooling curves of A356 alloy and its composites reinforced by 15vol% SiC_p, and observed a higher liquidus temperature for the latter than the unreinforced A356 alloy. Furthermore, investigations by Egizabal [19] revealed that TiB_2 particles change the solidification curve of the alloy, with an early initiation of solidification due to a decrease in the undercooling temperature and also a reduction in solidification time. The addition of TiB_2 particles into the molten metal introduces more nucleation sites and thereby reduces the undercooling. Thus, the determined liquidus temperature of composite melt appears to be higher.

From earlier works, it is apparent that though a considerable amount of research has focused on the solidification characteristics of AMMCs, no study yet has focused on the prediction of solidification curves of A356–TiB_2 composites, especially related to the solid fraction and the temperature relationships of A356–TiB_2 *in-situ* composites for SSMP. Thus, the present work investigates the solid fraction vs. temperature relationships of A356–TiB_2 *in-situ* composites.

2. Experimental

2.1. Materials

A commercial A356 alloy and A356–$x$$TiB_2$ (x = 2.5wt%, 5wt%) *in-situ* composites, synthesized by the flux-assisted synthesis (FAS) technique, were used in the present study. The chemical composition of the A356 alloy is shown in Table 1.

Table 1. Chemical composition of A356 alloy used in the present investigation wt%

Alloy	Si	Mg	Fe	Cu	Mn	Al
A356	6.87	0.297	0.12	0.01	0.003	92.70

2.2. Processing of A356–TiB_2 in-situ composites

The A356–$x$$TiB_2$ (x = 2.5wt% and 5wt% that are equivalent to 1.7vol% and 3.3vol%, respectively) *in-situ* composites were fabricated by the FAS technique. The K_2TiF_6 and KBF_4 halide salts undergo an exothermic, *in-situ* reaction with a molten Al–7Si alloy to create titanium–diboride (TiB_2) dispersoids in the melt. Initially, the appropriate amount of Al–50Si master alloy and commercial pure aluminum (CPAL) was molten in a graphite crucible in a resistance furnace for the preparation of the Al–7Si alloy. The melt was kept at a temperature of 800°C. Thereafter, salts were added and stirred every 10 min for a homogenous formation and distribution of TiB_2 particles. After a reaction time of 1 h, the dross floating on the top of the melt was decanted and the appropriate amount of Al–20Mg master alloy was added, in order to make the net composition of the composite to Al–7Si–0.3Mg–5TiB_2. A schematic diagram for the synthesis of the *in-situ* composites is shown in Fig. 1 and further details of the FAS technique can be found elsewhere [10–12].

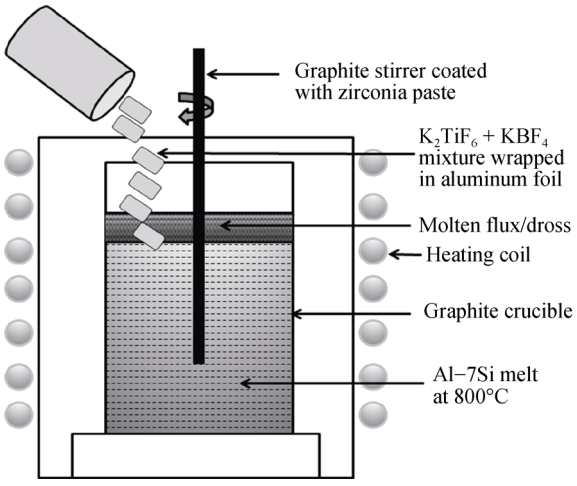

Fig. 1. Schematic diagram of A356–TiB_2 composite synthesis.

2.3. Cooling slope casting process

The cooling slope (CS) casting process was employed as a feedstock production method for both the alloy and com-

posites. The A356 alloy and A356–TiB_2 composites were melted at 720°C and 800°C, respectively, in a resistance furnace.

It was previously reported by Mandal *et al.* [11] that the reaction of K_2TiF_6 and KBF_4 halide salts with the molten aluminum alloy takes place completely at a reaction temperature of 800°C for 60 min. The melt was then degassed with 1wt% hexachloroethane, and inoculated with Al–5Ti–1B and Al–10Sr master alloys, in accordance with standard commercial practice. The melt was then left to cool to the desired pouring temperature of 640°C. The CS casting experiments involved pouring the molten A356 alloy and A356–TiB_2 composites over a 50-mm wide and 400-mm long inclined mild steel plate into a permanent mold with a 30-mm diameter and a 135-mm depth. The cooling plate was adjusted to 60° with respect to the horizontal plane and was cooled by water circulation underneath. The water circulation flow rate was kept a constant of 2 L/min throughout the experiments. The surface of the plate was coated with a thin layer of zirconia paste to avoid sticking the melt to the plate and to facilitate a trouble-free melt flow. A pre-heated graphite funnel was used as a pouring cup and a graphite cone allowed the melt to more easily fill in the mold. The molten metal started solidifying on the cooled plate and completely solidified in the mold. The temperatures were monitored with a K-type thermocouple fixed at the start and exit of the slope. The experimental setup of the CS casting process is shown in Fig. 2 and the experimental parameters used in the present study are given in Table 2. The composites were subsequently characterized by X-ray diffraction (XRD), using Cu K_α radiation (wavelength λ =0.154 nm) in an X-ray diffractometer to identify the phases.

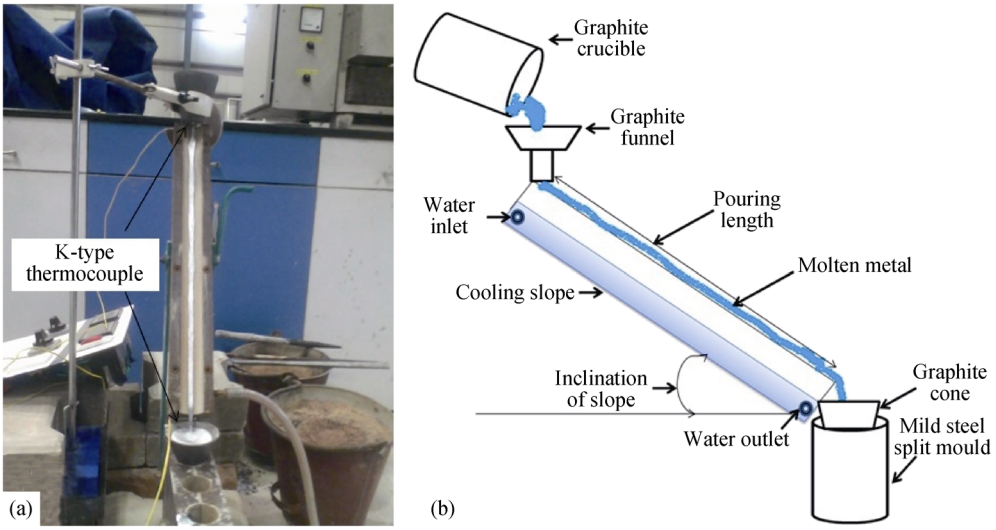

Fig. 2. Cooling slope casting: (a) experimental setup; (b) schematic illustration.

Table 2. Experimental conditions of cooling slope casting

Cooling slope dimensions	Length = 400 mm, width = 50 mm
Material of plate	Mild steel
Dimensions of plate	12.5 mm × 50 mm × 400 mm
Coating on the inclined plate	Zirconia paste
Pouring temperatures	640°C
CS plate angle	60°
Material of mould	Mild steel
Dimensions of mould	ϕ30 mm × 135 mm

2.4. Differential thermal analysis (DTA)

DTA was performed on the base alloy and composite specimens using a Perkin Elmer Pyris Diamond (TG-DTA) instrument. Specimens with 4-mm discs and weighing 10 mg were employed for the analysis. In the DTA technique, the alloy and composite specimens were remelted to 700°C, at a heating rate of 10°C·min^{-1}, and subsequently cooled to an ambient temperature at 10°C·min^{-1}. The interfacial reactions were quantified during continuous cooling experiments. The solid fraction (f_s) is defined as the percentage of the solid phase formed between the equilibrium and/or non-equilibrium liquidus (T_L) and solidus (T_S) temperatures in a solidifying melt of metal, alloys and metal matrix composites [20]. The thermal analysis results were then used to estimate the f_s of the alloys and the composites at varying temperatures, expressed numerically as a value in the range of 0 to 1.

3. Results and discussion

The XRD pattern in Fig. 3(a) clearly shows the presence of TiB_2 particles in A356–$x$$TiB_2$ (x = 2.5wt% and 5wt %)

composites. Fig. 3(b) shows the extracted TiB_2 particles from the A356–5TiB_2 composite, obtained by the chemical dissolution technique. Furthermore, the complete absence of intermediate products, such as Al_3Ti and AlB_2, is evident from the XRD patterns (Fig. 3(b)). This suggests the presence of only TiB_2 particles in the A356–5TiB_2 composite, thus confirming the complete reaction of K_2TiF_6 and KBF_4 halide salts with the molten aluminum alloy.

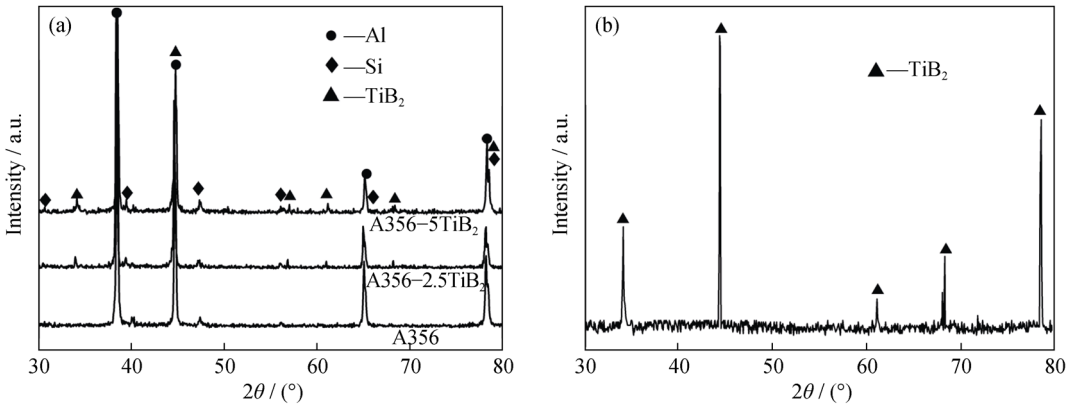

Fig. 3. XRD patterns of (a) A356 alloy and A356–TiB_2 composites and (b) extracted TiB_2 particles from A356–5TiB_2 composite.

Solidification of Al–7Si–Mg alloys has been well-documented by Backerud *et al.* [21] and the typical solidification sequence for this alloy is presented in Table 3.

Table 3. Solidification reactions observed in Al–7Si–Mg alloys [21]

Reaction No.	Reactions	Suggested start temperature / °C
1	L → α-Al dendrites	611–614
2	L → α-Al + Si	577
3a	L → α-Al + Si + Al_5FeSi	575
3b	L+Al_5FeSi → α-Al + Si + $Al_8FeMg_3Si_6$	567
4	L → α-Al + Si + Mg_2Si	555
5	L → α-Al + Si + Mg_2Si + $Al_8FeMg_3Si_6$	550–554

The DTA cooling curves of the alloy and composites in Fig. 4 show two major peaks corresponding to the precipitation of two phases as temperatures decreased. However, the phases corresponding to the reactions 3a, 3b, 4, and 5 in Table 3 could not be detected by DTA as the extent of these transformations might be a function of the cooling rate and Mg/Fe content. Peak 1 corresponds to the precipitation reaction of α-Al, while peak 2 corresponds to the nucleation and growth of Al–Si eutectic. Similar peaks were noticed earlier on the solidification behavior of Al–7%Si–Mg casting alloys [22].

In the current work, a ternary peak, which refers to the precipitation of multiphase eutectic α-Al + Si + Mg_2Si reactions in the DTA curves of the A356 alloy, is absent for a scan rate of 10°C·min^{-1}. However, these results are in agreement with that for a similar scan rate of 10°C·min^{-1} reported in the literature [15]. Moreover, the presence of a multiphase peak was visible for lower cooling rates of about 2.5°C·min^{-1} and 0.5°C·min^{-1}, as reported in the literature [15]. Moreover, it is assumed that the influence of Mg (A356 Al alloys contain 0.3wt% Mg) on the liquidus temperature is negligible, as previously reported [23]. The absence of a ternary α-Al + Si + Mg_2Si reaction in the DTA curves of A356–TiB_2 composites is due the influence of TiB_2 on Mg, which depresses the peak [10–11].

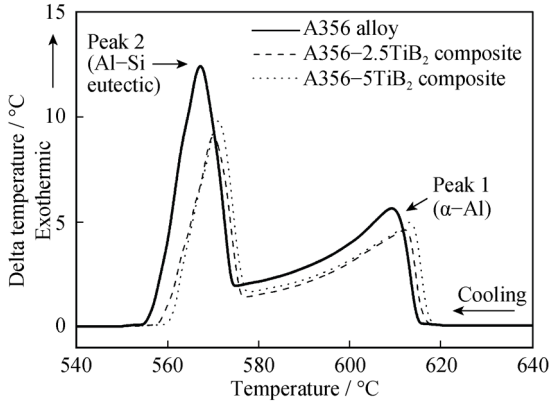

Fig. 4. DTA cooling curves of A356 alloy and A356–TiB_2 composites.

From the DTA cooling curves (Fig. 4), the liquidus (T_L), eutectic (T_E), and solidus (T_S) temperatures of the A356 alloy and its composites are summarized in Table 4.

It has been observed from the cooling characteristics, that the liquidus and solidus temperature of the base alloy are in agreement with the literature [24]. However, there is a slight decrease in the eutectic temperature of the alloy. Employing the DTA, it was observed that there is a shift in the liquidus

temperature of the A356–xTiB$_2$ composites, by 2°C and 3°C for x = 2.5wt% and 5wt%, respectively, and a shift in the solidus temperature of the composites by 3 and 5°C, respectively, compared with the base alloy. These changes in the solidus and liquidus temperatures resulted in a decrease in the solidification intervals of A356–xTiB$_2$ (x = 2.5wt% and 5wt%) composites by 1 and 2°C, respectively, with respect to the base alloy. This was due to an incorporation of TiB_2 in the alloy. These results are in agreement with those stated in the literature [19].

Table 4. DTA cooling characteristics of A356 alloy and A356–TiB_2 composites

Alloy/Composite	Temperature of peak 1 (primary α-Al dendrites) / °C		Temperature of peak 2 (Al–Si eutectic) / °C		Solidus temperature, T_S / °C
	Onset/Liquidus (T_L)	Peak	Onset	Peak/Eutectic (T_E)	
A356	615	609	574	567	555
A356–2.5TiB_2	617	612	576	570	558
A356–5TiB_2	618	613	577	571	560

The degree of undercooling is determined as the difference between the highest and lowest temperatures recorded during a solidification reaction. Details regarding metallurgical events during solidification were well-documented and reported in the literature [19–21]. In the current study, the undercooling temperatures during the eutectic reaction (T_E) of A356–5TiB$_2$ (x = 2.5wt% and 5wt%) composites (577°C – 571°C = 6°C) were found to be 1°C, relative to 7°C (574°C – 567°C = 7°C) in the unreinforced A356 alloy. This was attributed to the TiB_2 particles, which act as a grain refiner and reduce the effect of undercooling. Moreover, the eutectic temperature (T_E) of A356–xTiB$_2$ composites was found to be 570°C and 571°C for x = 2.5wt% and 5wt%, respectively, which was much higher than that of 567°C for the base alloy.

The Scheil equation [25] was used to estimate the solid fraction (f_s) using Eq. (1) below.

$$f_s = \frac{1}{1-k_p} \cdot \frac{T-T_L}{T-T_M} \quad (1)$$

For the Scheil equation, T_L is the liquidus temperature of the alloy/composite, T_M is the melting point of pure aluminum, T is the temperature at the solid fraction f_s, and k_p is the partition coefficient, which is taken as 0.13 [25]. The solidification curves of the A356 alloy and A356–TiB_2 composites are plotted in Fig. 5.

From the solidification curves of the A356 alloy and A356–TiB_2 composites, the base alloy has an f_s value of 0.5, which corresponds to 580°C, in agreement with the literature [24]. However, the solidification curves of A356–xTiB$_2$ (x = 2.5wt% and 5wt%) composites indicate that at f_s = 0.5, the temperatures correspond to 583°C and 585°C, respectively. A similar trend was noticed for solid fraction values in the range of 0–1, for which the corresponding temperatures of the composites were higher relative to that of the unreinforced alloy. The increase in composite temperature values with respect to f_s values was in agreement with the literature [26] when the composites were thixoformed at higher temperatures, compared to the base alloy.

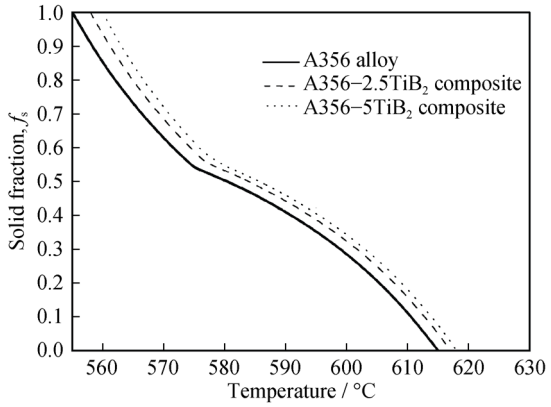

Fig. 5. Solidification curves of A356 alloy and A356–TiB_2 composites.

4. Conclusions

(1) The solidification interval of A356–TiB_2 composites was found to be marginally lower than that of the A356 alloy. Also, the solidification began earlier for composites, as compared to the base alloy.

(2) The undercooling temperatures experienced during the eutectic reaction of A356–5TiB$_2$ (x = 2.5wt% and 5wt%) composites were lower compared to that of the unreinforced alloy. This was due to the nucleating sites provided by the *in-situ* TiB_2 particles.

(3) The eutectic temperatures of the A356–xTiB$_2$ (x = 2.5wt% and 5wt%) composites were higher than that of the base alloy by 3°C and 4°C, respectively.

Acknowledgements

The authors gratefully acknowledge the financial support

from the Indian Institute of Technology Bhubaneswar under the SEED project grant for fabricating the "cooling slope casting" experimental setup. Further, the support extended by Central Research Facility (CRF), Indian Institute of Technology Kharagpur, toward the facility for conducting DTA experiments is gratefully acknowledged.

References

[1] S. Tahamtan, M.A. Golozar, F. Karimzadeh, and B. Niroumand, Microstructure and tensile properties of thixoformed A356 alloy, *Mater. Charact.*, 59(2008), No. 3, p. 223.

[2] H.V. Atkinson, Modelling the semisolid processing of metallic alloys, *Prog. Mater. Sci.*, 50(2005), No. 3, p. 341.

[3] Z. Fan, Semisolid metal processing, *Int. Mater. Rev.*, 47(2002), No. 2, p. 1.

[4] M.H. Robert, E.J. Zoqui, F. Tanabe, and T. Motegi, Producing thixotropic semi-solid A356 alloy: microstructure formation x forming behaviour, *J. Achiev. Mater. Manuf. Eng.*, 20(2007), No. 1-2, p. 19.

[5] T. Haga and S. Suzuki, Casting of aluminum alloy ingots for thixoforming using a cooling slope, *J. Mater. Process. Technol.*, 118(2001), No. 1-3, p. 169.

[6] Y. Birol, A357 thixoforming feedstock produced by cooling slope casting, *J. Mater. Process. Technol.*, 186(2007), No. 1-3, p. 94.

[7] M.A. Bayoumi, M.I. Negm, and A.M. El-Gohry, Microstructure and mechanical properties of extruded Al–Si alloy (A356) in the semi-solid state, *Mater. Des.*, 30(2009), No. 10, p. 4469.

[8] M. Paes and E.J. Zoqui, Semi-solid behavior of new Al–Si–Mg alloys for thixoforming, *Mater. Sci. Eng. A*, 406(2005), No. 1-2, p. 63.

[9] S. Lakshmi, L. Lu, and M. Gupta, *In situ* preparation of TiB_2 reinforced Al based composites, *J. Mater. Process. Technol.*, 73(1998), No. 1-3, p. 160.

[10] A. Mandal, R. Maiti, M. Chakraborty, and B.S. Murty, Effect of TiB_2 particles on aging response of Al–4Cu alloy, *Mater. Sci. Eng. A*, 386(2004), No. 1, p. 296.

[11] A. Mandal, M. Chakraborty, and B.S. Murty, Ageing behaviour of A356 alloy reinforced with *in-situ* formed TiB_2 particles, *Mater. Sci. Eng. A*, 489(2008), No. 1-2, p. 220.

[12] S. Kumar, V. Subramanya Sarma, and B.S. Murty, A statistical analysis on erosion wear behaviour of A356 alloy reinforced with *in situ* formed TiB_2 particles, *Mater. Sci. Eng. A*, 476(2008), No. 1-2, p. 333.

[13] C.S. Ramesh, S.K. Jagadeesh, and R. Keshavamurthy, Solidification studies on sand cast Al 6061–SiC_p composites, *J. Alloys Compd.*, 509(2011), Suppl. 1, p. S371.

[14] S.C. Jeng and S.W. Chen, The solidification characteristics of 6061 and A356 aluminum alloys and their ceramic particle-reinforced composites, *Acta Mater.*, 45(1997), No. 12, p. 4887.

[15] Y. Birol, Solid fraction analysis with DSC in semi-solid metal processing, *J. Alloys Compd.*, 486(2009), No. 1-2, p. 173.

[16] G. Klancnik, J. Medved, and P. Mrvar, Differential thermal analysis (DTA) and differential scanning calorimetry (DSC) as a method of material investigation, *RMZ Mater. Geoenviron.*, 57(2010), No. 1, p. 127.

[17] S. Gowri and F.H. Samuel, Effect of cooling rate on the solidification behavior of Al–7 Pct Si–SiC_p metal-matrix composites, *Metall. Trans. A*, 23(1992), No. 12, p. 3369.

[18] H. Kaufmann, E. Neuworth, J. Larcher, and H. Pacyna, Quality control for casting particulate reinforced aluminium alloys, [in] *Proceedings of* 3*rd International Conference on Aluminium Alloys,* Trondheim, Norway, 1992, p. 81.

[19] P. Egizabal, *Influence of Titanium Diboride (TiB_2) Particles on the Microstructure and Properties of Reinforced Al–Si7Mg*0.3 *and Al–Cu5MgTi Alloys for Plaster Casting Applications* [Dissertation], University of Bordeaux, France, 2007, p. 176.

[20] P. Marchwica, J.H. Sokolowski, and W.T. Kierkus, Fraction solid evolution characteristics of AlSiCu alloys: dynamic baseline approach, *J. Achiev. Mater. Manuf. Eng.*, 47(2011), No. 2, p. 115.

[21] L. Backerud, G. Chai, and J. Tamminen, *Solidification Characteristics of Aluminum Alloys*, American Foundrymen's Society, 1990, p. 128.

[22] Z.W. Chen, J.S. Li, W.Q. Jie, L. Liu, and H.Z. Fu, Solidification behaviour of Al–7%Si–Mg casting alloys, *Trans. Nonferrous Met. Soc. China*, 15(2005), No. 1, p. 40.

[23] K.R. Ravi, R.M. Pillai, B.C. Pai, and M. Chakraborty, A novel approach for extracting and characterizing interfacial reaction products in Al–SiC_p composites, *Metall. Mater. Trans. A*, 38(2007), p. 1666.

[24] P. Das, S.K. Samanta, H. Chattopadhyay, and P. Dutta, Effect of pouring temperature on cooling slope casting of semi-solid Al–Si–Mg alloy, *Acta Metall. Sin. Eng. Lett.*, 25(2012), No. 5, p. 329.

[25] J. Wannasin and S. Thanabumrungkul, Development of a semi-solid metal processing technique for aluminium casting applications, *Songklanakarin J. Sci. Technol.*, 30(2008), No. 2, p. 215.

[26] I.G. Siddhalingeshwar, M.A. Herbert, M. Chakraborty, and R. Mitra, Effect of mushy state rolling on age-hardening and tensile behavior of Al–4.5Cu alloy and in situ Al–4.5Cu–5TiB_2 composite, *Mater. Sci. Eng. A*, 528(2011), No. 3, p. 1787.